Transition Met Chem (2014) 39:127–133
DOI 10.1007/s11243-013-9781-x

Kinetic characterization of the interactions of *trans*-dichloro-platinum(IV) anticancer prodrugs and a model compound with thiosulfate

Jingran Dong · Shuying Huo · Changying Song · Shigang Shen · Yanli Ren · Tiesheng Shi

Received: 10 August 2013 / Accepted: 31 October 2013 / Published online: 9 November 2013

Abstract Sodium thiosulfate has been utilized as a rescuing agent for relief of the toxic effects of cisplatin and carboplatin. In this work, we characterized the kinetics of reactions of the *trans*-dichloro-platinum(IV) complexes *cis*-$[Pt(NH_3)_2Cl_4]$, ormaplatin $[Pt(dach)Cl_4]$ and *trans*-$[PtCl_2(CN)_4]^{2-}$ (anticancer prodrugs and a model compound) with thiosulfate at biologically important pH. An overall second-order rate law was established for the reduction of *trans*-$[PtCl_2(CN)_4]^{2-}$ by thiosulfate, and varying the pH from 4.45 to 7.90 had virtually no influence on the reaction rate. In the reactions of thiosulfate with *cis*-$[Pt(NH_3)_2Cl_4]$ and with $[Pt(dach)Cl_4]$, the kinetic traces displayed a fast reduction step followed by a slow substitution involving the intermediate Pt(II) complexes. The reduction step also followed second-order kinetics. Reductions of *cis*-$[Pt(NH_3)_2Cl_4]$ and $[Pt(dach)Cl_4]$ by thiosulfate proceeded with similar rates, presumably due to their similar configurations, whereas the reduction of *trans*-$[PtCl_2(CN)_4]^{2-}$ was about 1,000 times faster. A common reduction mechanism is suggested, and the transition state for the rate-determining step has been delineated. The activation parameters are consistent with transfer of Cl^+ from the platinum(IV) center to the attacking thiosulfate in the rate-determining step.

J. Dong · S. Huo · C. Song · S. Shen · Y. Ren · T. Shi (✉)
College of Chemistry and Environmental Science and, Key Laboratory for Medicinal Chemistry and Molecular Diagnostics (the Ministry of Education), Hebei University, Baoding 071002, Hebei Province, People's Republic of China
e-mail: rock@hbu.edu.cn

Introduction

Among the chemotherapeutic drugs, platinum complexes currently play a central role [1–4]; of those complexes, cisplatin and carboplatin are used worldwide. However, these drugs have several side effects, most notably nephrotoxicity and ototoxicity. As a consequence, the design and synthesis of a new generation of platinum-based anticancer agents, including some Pt(IV) complexes, are of current interest with a goal of overcoming or minimizing the side effects [1–3]. Progress in this direction appears to be slow [1–3] owing to the poor understanding of anticancer mechanisms. On the other hand, some rescuing agents have been discovered for cisplatin and carboplatin, which give some relief from their side effects [4–7]. These rescuing agents, encompassing sodium thiosulfate, amifostine, *N*-acetyl-L-cysteine, D-methionine, and ebselen, are typical antioxidants [4]. The most promising is probably sodium thiosulfate, currently entering into phase III trials [4]. Due to the importance of sodium thiosulfate in relieving the toxic effects of cisplatin and carboplatin, the interactions of thiosulfate with cisplatin and carboplatin have been investigated [8–10].

Some *trans*-dichloro-platinum(IV) complexes have been found to possess certain types of biological functions. These include anticancer active agents such as the prototype ormaplatin, as well as highly selective reagents for the formation of intramolecular disulfide bonds in peptides and proteins [11–16]. Platinum(IV) anticancer agents are often regarded as prodrugs, owing to their ease of reduction, which is often accompanied by the loss of their axially coordinated ligands [2]. The interactions of Pt(IV) anticancer agents with thiosulfate have, however, not been exploited. In this work, we report our kinetic results on the interactions of thiosulfate with *trans*-dichloro-Pt(IV)

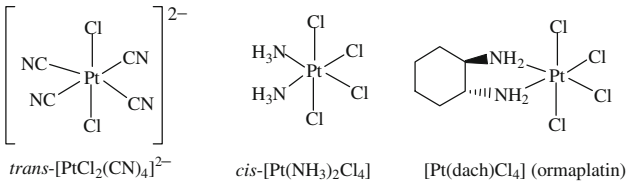

trans-$[PtCl_2(CN)_4]^{2-}$ *cis*-$[Pt(NH_3)_2Cl_4]$ [Pt(dach)Cl_4] (ormaplatin)

Scheme 1 Structures of Pt(IV) anticancer prodrugs and model compound

prodrugs *cis*-$[Pt(NH_3)_2Cl_4]$ and ormaplatin and a model compound *trans*-$[PtCl_2(CN)_4]^{2-}$ (structures are given in Scheme 1).

Experimental

Instrumentation

The UV–vis spectra were recorded on a TU-1900 spectrophotometer (Beijing Puxi, Inc., Beijing, China) using 1.00 cm quartz cells. An Applied Photophysics SX-20 stopped-flow spectrometer (Applied Photophysics Ltd., Leatherhead, UK) was used for kinetic runs and for recording time-resolved spectra. An Accumet Basic AB15 Plus pH meter equipped with an Accumet® combination pH electrode (Fisher Scientific, Pittsburgh, PA, USA) was used for pH measurements. The electrode was calibrated just before the pH measurements by the use of standard buffers of pH 4.00, 7.00, and 10.00, also from Fisher Scientific.

Chemicals and solutions

$K_2[Pt(CN)_4]\cdot 3H_2O$ and *cis*-$[Pt(NH_3)_2Cl_4]$ were obtained from Sigma-Aldrich. Potassium tetrachloroplatinate(II), (1R,2R)-(-)-1,2-diaminocyclohexane (dach), sodium thiosulfate, acetic acid, sodium acetate, sodium chloride, hydrochloric acid, sodium dihydrogen phosphate, disodium hydrogen phosphate, sodium perchlorate, all of analytical grade, were purchased either from Fisher Scientific or from Alfa Aesar and used without further purification. $K_2[PtCl_2(CN)_4]$ was synthesized using the reported method [17]; the UV–vis spectra of aqueous solutions prepared from $K_2[PtCl_2(CN)_4]$ are in excellent agreement with that reported earlier for *trans*-$[PtCl_2(CN)_4]^{2-}$ [18]. Ormaplatin (tetraplatin, [Pt(dach)Cl_4]) was synthesized by the procedure described in the literature [19]; elemental and mass spectrometric analyses confirmed the successful synthesis. Doubly distilled water was used to prepare all the solutions.

Buffers of acetic acid/sodium acetate and NaH_2PO_4/Na_2HPO_4 (with concentrations of 0.2–0.3 M) were prepared to cover a pH range of 4.45–7.90; all the buffers, which contained 2 mM EDTA and 0.10 M NaCl, were adjusted to an ionic strength (μ) of 1.0 M with sodium perchlorate. The addition of NaCl to the buffers was to suppress the hydrolysis of the platinum(IV) complexes, while EDTA was added as a complexing agent for trace metal ions such as Cu(II), in order to eliminate their catalytic effects in autooxidation of thiosulfate [20, 21]. Stock solutions of 1.0 mM *trans*-$[PtCl_2(CN)_4]^{2-}$, *cis*-$[Pt(NH_3)_2Cl_4]$, and [Pt(dach)Cl_4] were prepared by dissolving the appropriate amount of each Pt(IV) complex in a solution containing 0.90 M $NaClO_4$, 0.09 M NaCl, and 0.01 M HCl. The stock solutions of *cis*-$[Pt(NH_3)_2Cl_4]$ and [Pt(dach)Cl_4] were prepared afresh every day.

Kinetic experiments

For kinetic studies, solutions of platinum(IV) and thiosulfate were prepared by adding an appropriate amount of the Pt(IV) stock solution or of thiosulfate to a specific buffer solution. Those solutions were flushed for 10 min with nitrogen before loading into the stopped-flow machine and were only used for a maximum of 2 h. Reactions were initiated by mixing equal volumes of platinum(IV) and thiosulfate solutions directly in the stopped-flow machine and were followed under pseudo-first-order conditions with thiosulfate being at least 10-fold excess.

Results and discussion

Reduction of *trans*-$[PtCl_2(CN)_4]^{2-}$

The kinetics of the reaction between *trans*-$[PtCl_2(CN)_4]^{2-}$ and thiosulfate was briefly studied by Fanchiang et al. [22] at 25 °C and $\mu = 0.10$ M in narrow ranges of pH and $[S_2O_3^{2-}]$ ($6.6 \leq$ pH ≤ 7.6, 0.408 mM $\leq [S_2O_3^{2-}] \leq 1.02$ mM). In the present work, the reaction was investigated at $\mu = 1.0$ M and in a temperature range of 25.0–40.0 °C over a much wider pH range. Time-resolved spectra for the reaction are displayed in Fig. 1. The growing peak at 255 nm is ascribed to the formation of $[Pt(CN)_4]^{2-}$. Two clear isosbestic points at 242.0 and 286.9 nm are found from the spectra in Fig. 1, which are indicative of a simple conversion of *trans*-$[PtCl_2(CN)_4]^{2-}$ to $[Pt(CN)_4]^{2-}$, namely a redox reaction, whereas the oxidation of thiosulfate does not make any noticeable contribution to the overall spectral changes observed in Fig. 1. No subsequent reaction was detected after the reduction of *trans*-$[PtCl_2(CN)_4]^{2-}$, in line with the fact that $[Pt(CN)_4]^{2-}$ is robust.

Under pseudo-first-order conditions with $[S_2O_3^{2-}] \geq 10[Pt(IV)]$, the kinetic traces at 255 nm could be simulated very well by single exponentials, suggesting that the reaction is indeed first order in $[PtCl_2(CN)_4^{2-}]$. The observed first-order rate constants, k_{obsd}, were thus

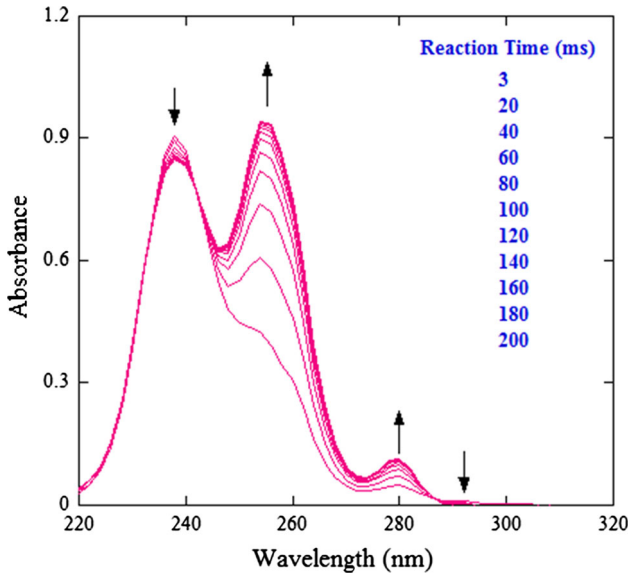

Fig. 1 Time-resolved spectra for reaction between *trans*-$[PtCl_2(CN)_4]^{2-}$ and thiosulfate in pH 7.34 phosphate buffer under the conditions: [Pt(IV)] = 0.083 mM, $[S_2O_3^{2-}] = 1.00$ mM, $\mu = 1.0$ M and 25.0 °C. The time (in milliseconds) for each spectrum after mixing is shown in the figure

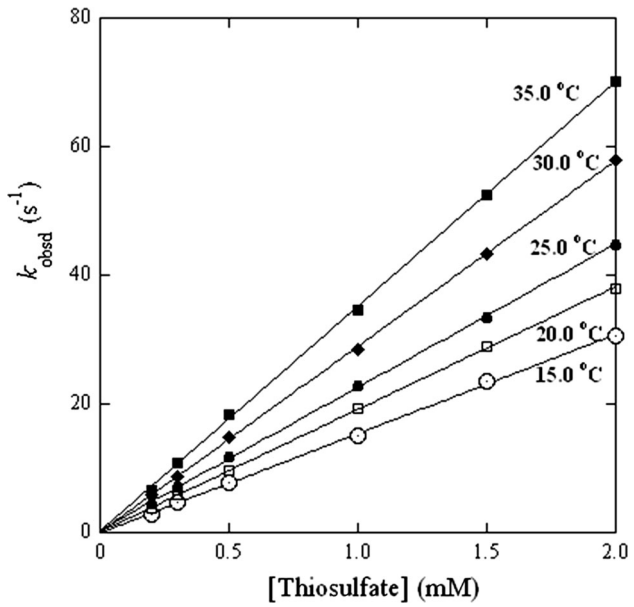

Fig. 2 Pseudo-first-order rate constants, k_{obsd}, as a function of [thiosulfate] for the reduction of *trans*-$[PtCl_2(CN)_4]^{2-}$ in phosphate. Reaction conditions: [Pt(V)] = 0.05 mM, pH = 7.34 and $\mu = 1.0$ M

obtained from the simulations; standard deviations from 3 to 5 replicate runs were usually much smaller than 5 %.

The influence of $[S_2O_3^{2-}]$ on the reaction rate was studied in the region 0.20 mM $\leq [S_2O_3^{2-}] \leq$ 2.0 mM; plots of k_{obsd} versus $[S_2O_3^{2-}]$ were linear and passed through the origin (Fig. 2), indicating that the reaction is also first order in $[S_2O_3^{2-}]$. Hence, Eq. 1 can express the rate law.

Table 1 Influences of changing pH on the observed second-order rate constants k for the reduction of *trans*-$[PtCl_2(CN)_4]^{2-}$ by thiosulfate at 25.0 °C and $\mu = 1.0$ M

pH	k (M^{-1} s^{-1})
4.45	$(2.60 \pm 0.06) \times 10^4$
5.12	$(2.74 \pm 0.08) \times 10^4$
5.62	$(2.76 \pm 0.05) \times 10^4$
6.10	$(2.54 \pm 0.06) \times 10^4$
6.55	$(2.30 \pm 0.05) \times 10^4$
7.10	$(2.25 \pm 0.06) \times 10^4$
7.34	$(2.22 \pm 0.06) \times 10^4$
7.90	$(2.36 \pm 0.09) \times 10^4$

Measured under the conditions of [Pt(IV)] = 0.02 − 0.05 mM; $[S_2O_3^{2-}] = 0.20 - 2.00$ mM and 255 nm

$$d\left[Pt(CN)_4^{2-}\right]\Big/dt = k_{obsd}\left[PtCl_2(CN)_4^{2-}\right] = k\left[S_2O_3^{2-}\right]\left[PtCl_2(CN)_4^{2-}\right] \quad (1)$$

The impact of solution pH on the second-order rate constant k was investigated in buffers between 4.45 $\leq$ pH $\leq$ 7.90; the results are summarized in Table 1. The pH has virtually no influence on the reaction rate, coinciding with the fact that both *trans*-$[PtCl_2(CN)_4]^{2-}$ and $S_2O_3^{2-}$ have no protolytic equilibria in the pH region studied (thiosulfuric acid has pK_a values of 0.6 and 1.6 at 25 °C). Therefore, the previously proposed reaction mechanism, as described by Eqs. (2) and (3) [22], is very reasonable. Our time-resolved spectra and rate law strongly support this mechanism.

$$\left[PtCl_2(CN)_4\right]^{2-} + S_2O_3^{2-} \xrightarrow{k} \left[Pt(CN)_4\right]^{2-} + Cl^- + ClS_2O_3^- \quad (2)$$

$$ClS_2O_3^- + S_2O_3^{2-} \xrightarrow{\text{rapid}} S_4O_6^{2-} + Cl^- \quad (3)$$

The second-order rate constants were calculated from Fig. 1 at pH = 7.34 (biologically relevant pH), cf. Table 2. The activation parameters were calculated by means of the Eyring equation (Fig. 3; Table 2). The value of $k = (2.22 \pm 0.06) \times 10^4$ M^{-1} s^{-1} at 25.0 °C and $\mu = 1.0$ M obtained from the present work is in good agreement with that of $k = (8.5 \pm 0.25) \times 10^3$ M^{-1} s^{-1} at 25.0 °C and $\mu = 0.10$ M reported earlier [22] once the difference in ionic strength is taken into account.

Interaction of *cis*-$[Pt(NH_3)_2Cl_4]$ with thiosulfate

The UV–vis spectra of *cis*-$[Pt(NH_3)_2Cl_4]$ and $S_2O_3^{2-}$ in a phosphate buffer of pH 7.34 are given in Fig. 4; clearly, there is a significant absorption difference between the two reactants around 280 nm. Kinetic traces followed around 280 nm using the stopped-flow spectrometer showed a biphasic character. Figure 5 displays a typical trace,

Table 2 Second-order rate constants k and activation parameters for the reduction of *trans*-$[PtCl_2(CN)_4]^{2-}$, *cis*-$[Pt(NH_3)_2Cl_4]$, and $[Pt(dach)Cl_4]$ by thiosulfate at pH 7.34 and $\mu = 1.0$ M

Pt(IV)	t (°C)	k (M^{-1} s^{-1})	$\Delta H^{\ddagger}$ (kJ mol^{-1})	$\Delta S^{\ddagger}$ (J K^{-1} mol^{-1})
$[PtCl_2(CN)_4]^{2-}$	15.0	$(1.54 \pm 0.02) \times 10^4$	27.9 ± 1.4	–68 ± 5
	20.0	$(1.91 \pm 0.02) \times 10^4$		
	25.0	$(2.22 \pm 0.06) \times 10^4$		
	30.0	$(2.89 \pm 0.04) \times 10^4$		
	35.0	$(3.50 \pm 0.07) \times 10^4$		
$[Pt(NH_3)_2Cl_4]$	20.0	12.2 ± 0.2	60.5 ± 1.5	–18 ± 6
	25.0	17.5 ± 0.2		
	30.0	28.8 ± 0.5		
	35.0	41.3 ± 0.8		
	40.0	62.6 ± 0.9		
$[Pt(dach)Cl_4]$	25.0	13.4 ± 0.3	52.4 ± 1.3	–48 ± 5
	30.0	19.3 ± 0.4		
	35.0	27.1 ± 0.5		
	40.0	39.5 ± 0.8		

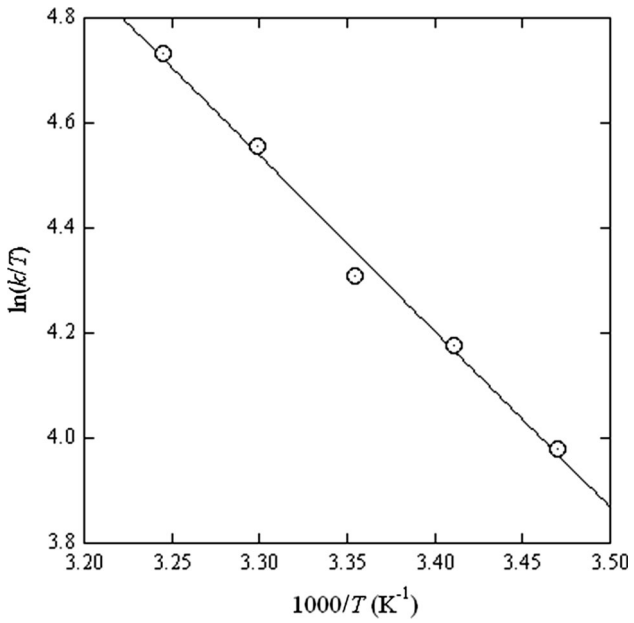

Fig. 3 Eyring's plot for the second-order rate constants k for the reduction of *trans*-$[PtCl_2(CN)_4]^{2-}$ by thiosulfate

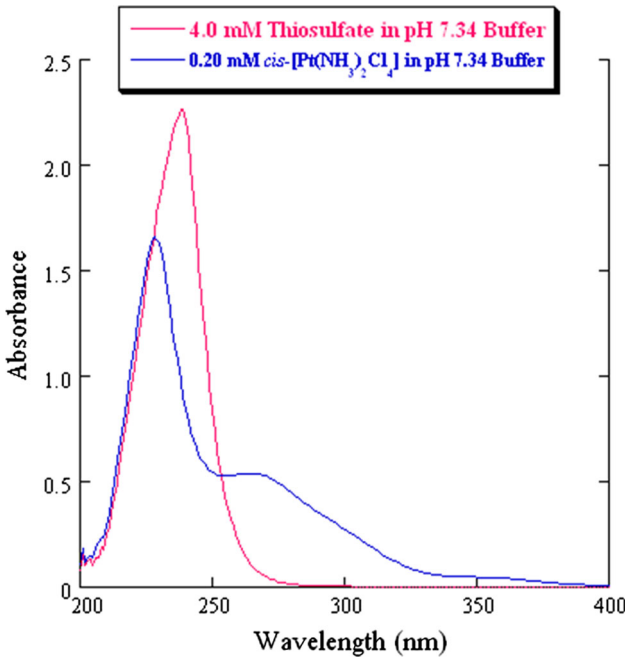

Fig. 4 UV–vis spectra of 0.2 mM *cis*-$[Pt(NH_3)_2Cl_4]$ and 4.0 mM thiosulfate in pH 7.34 phosphate buffer

obtained under pseudo-first-order conditions, showing that a fast reaction (the absorbance decrease part) is followed by a slow reaction (the absorbance increase part). The biphasic character suggests that the overall reaction may involve two consecutive first-order reactions as described by reaction (4) [23], where **A** represents *cis*-$[Pt(NH_3)_2Cl_4]$, while **B** and **C** pertain to the intermediate and final Pt complexes (vide infra).

$$\mathbf{A} \xrightarrow{k_f} \mathbf{B} \xrightarrow{k_s} \mathbf{C} \tag{4}$$

The kinetic trace in Fig. 5 was simulated using Eq. (5), where A and A_∞ are the absorbances at reaction time t and infinity; α and β are constants related to the initial

$$A = \alpha \exp(-k_f t) + \beta \exp(-k_s t) + A_\infty \tag{5}$$

concentration of the Pt(IV) complex, the molar absorptivities of species **A**–**C** and k_f and k_s [23]. The simulation resulted in a good fit, giving rise to two first-order rate

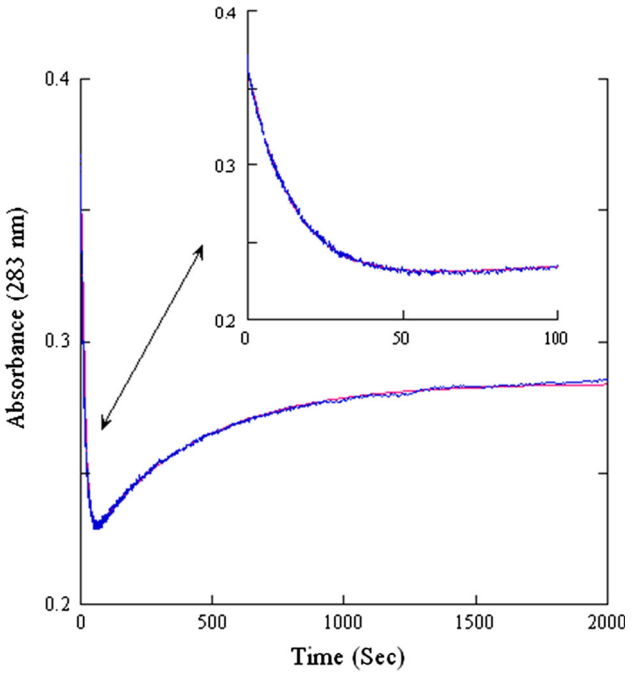

Fig. 5 A kinetic trace at 283 nm and 25.0 °C for the reaction of *cis*-$[Pt(NH_3)_2Cl_4]$ with thiosulfate in phosphate buffer (*blue dot line*). Conditions: [Pt(V)] = 0.2 mM, $[S_2O_3^{2-}]$ = 4.0 mM, pH = 7.34, and μ = 1.0 M. The smooth *red line* was resulted from the curve fitting of Eq. (5) to the experimental data by a nonlinear least-squares method. *Inset* enlarged scale for the kinetic trace in the region of 0–100 s. (Color figure online)

Table 3 Observed second-order rate constants of the fast reaction k_f and the slow reaction k_s for interaction between *cis*-$[Pt(NH_3)_2Cl_4]$ and thiosulfate in pH 7.34 solution at 25.0 °C and μ = 1.0 M

$[S_2O_3^{2-}]$ (mM)	k_{obsd} $(s^{-1})^a$	k_f $(s^{-1})^b$	k_s $(s^{-1})^b$
2.00	0.037 ± 0.003	0.031 ± 0.003	(3.7 ± 0. 4) × 10^{-4}
4.00	0.069 ± 0.004	0.069 ± 0.003	(2.4 ± 0. 4) × 10^{-3}
8.00	0.140 ± 0.005	0.135 ± 0.004	(4.4 ± 0. 6) × 10^{-3}
12.0	0.21 ± 0.01	0.20 ± 0.01	(9.1 ± 0.7) × 10^{-3}
20.0	0.35 ± 0.02	0.32 ± 0.02	0.016 ± 0.001

Measured under the conditions of [Pt(IV)] = 0.2 mM and 283 nm

[a] Obtained by one reaction

[c] Obtained by two reactions

constants k_f and k_s. Values of k_f and k_s as a function of $[S_2O_3^{2-}]$ measured at 25.0 °C are listed in Table 3.

On the other hand, the kinetic trace in Fig. 5 could be simulated separately if two half lives or less of the first reaction (absorbance decrease part) were used, such that the effect of the second reaction was negligible. Using this approach, the first reaction was well simulated by a single exponential, yielding the pseudo-first-order rate constants k_{obsd} (also listed in Table 3). There is good agreement between the values of k_{obsd} and k_f obtained from the two different simulations.

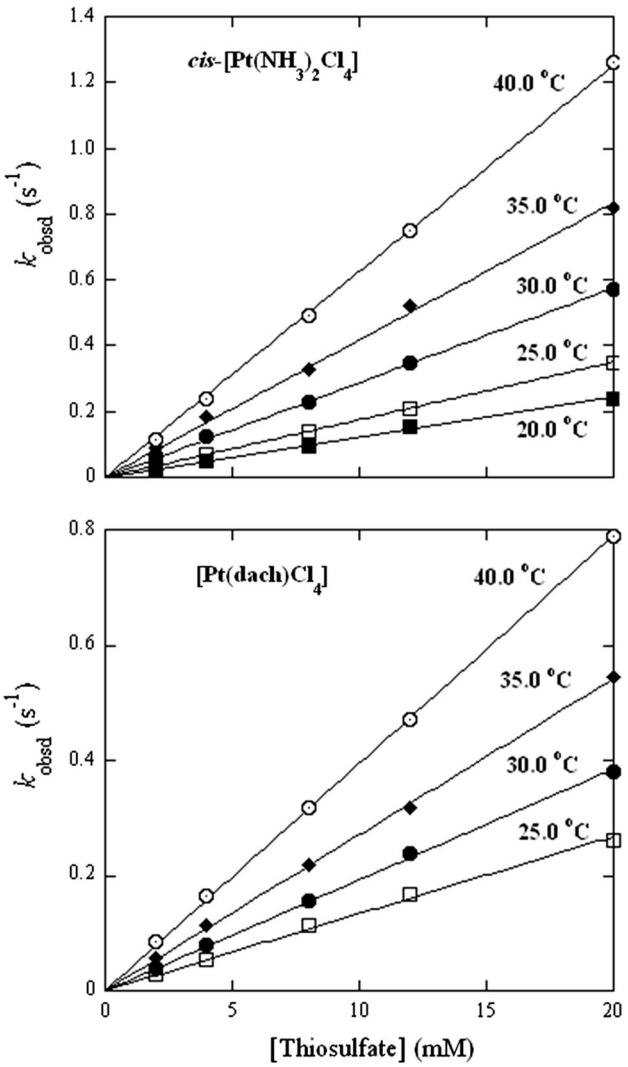

Fig. 6 Plots of k_{obsd} versus $[S_2O_3^{2-}]$ for the reductions of *cis*-$[Pt(NH_3)_2Cl_4]$ and $[Pt(dach)Cl_4]$ by thiosulfate in phosphate buffer. Reaction conditions: [Pt(V)] = 0.1–0.2 mM, pH = 7.34, and μ = 1.0 M

Subsequently, the first reaction was followed at several temperatures. Plots of k_{obsd} against $[S_2O_3^{2-}]$ are shown in Fig. 6; clearly, the first reaction follows an overall second-order kinetics, similar to the reduction of *trans*-$[PtCl_2(CN)_4]^{2-}$ by thiosulfate. Thus, the first reaction can be safely assigned to the reduction of *cis*-$[Pt(NH_3)_2Cl_4]$ to *cis*-$[Pt(NH_3)_2Cl_2]$ by thiosulfate. This assignment is substantiated by the substitution inertness of Pt(IV) complexes in general and by the rapidity of the first reaction. A rate law as shown in Eq. (6) can be established from the plots in Fig. 6:

$$-\mathrm{d}\left[Pt(NH_3)_2Cl_4\right]/\mathrm{d}t = k_{obsd}\left[Pt(NH_3)_2Cl_4\right] = k\left[S_2O_3^{2-}\right]\left[Pt(NH_3)_2Cl_4\right] \quad (6)$$

Second-order rate constants k for the reduction of *cis*-$[Pt(NH_3)_2Cl_4]$ by thiosulfate evaluated from Fig. 6 are given in Table 2. The corresponding activation parameters

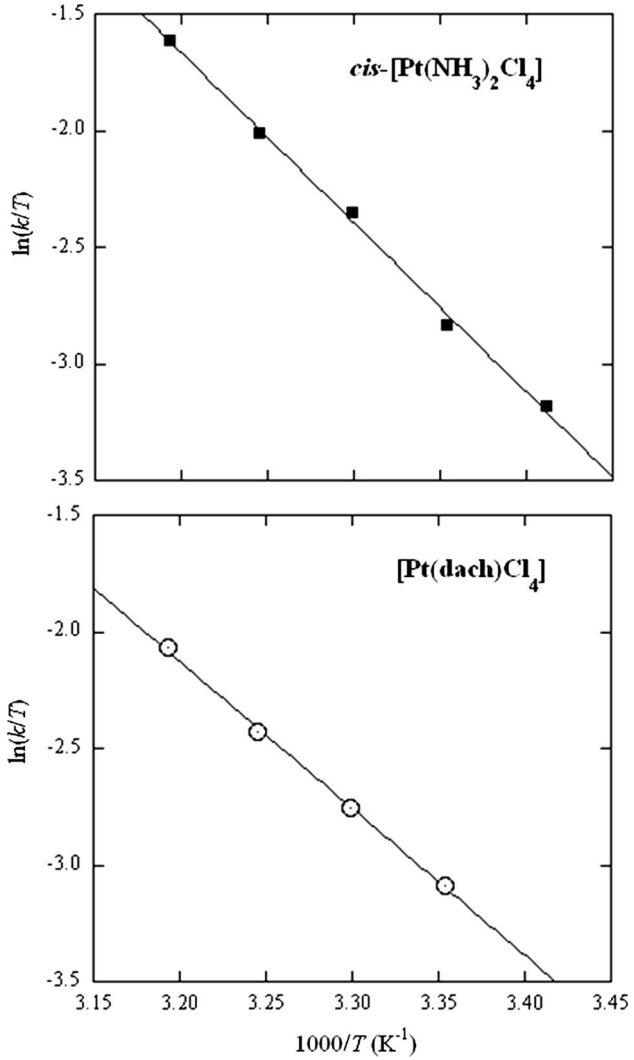

Fig. 7 Eyring's plots for the second-order rate constants k for the reductions of *cis*-$[Pt(NH_3)_2Cl_4]$ and $[Pt(dach)Cl_4]$ by thiosulfate

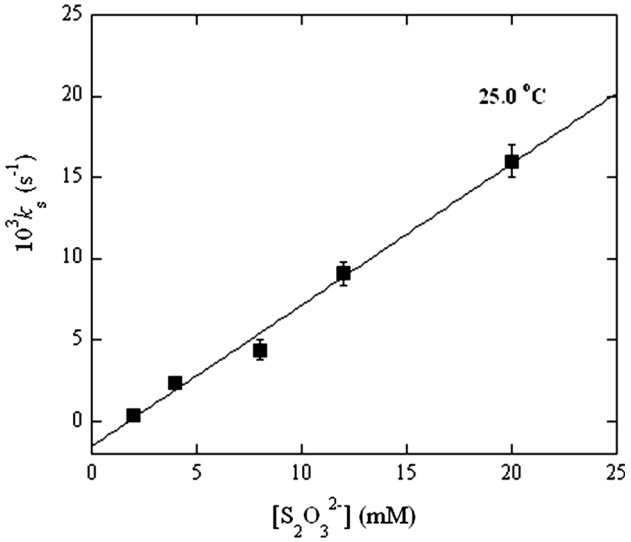

Fig. 8 Plot of k_s versus $[S_2O_3^{2-}]$ at 25.0 °C for the slow phase of the reaction (substitution reaction) between *cis*-$[Pt(NH_3)_2Cl_4]$ and thiosulfate

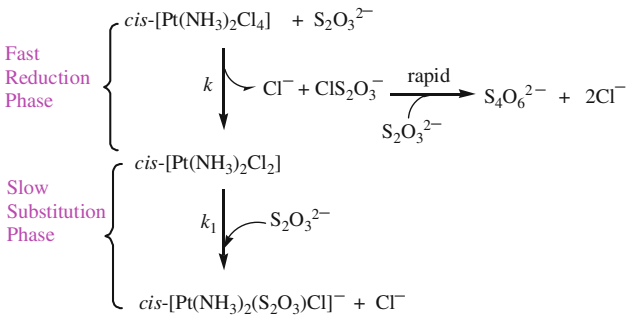

Scheme 2 The biphasic reaction mechanism for the interaction between *cis*-$[Pt(NH_3)_2Cl_4]$ and thiosulfate

calculated from the Eyring plot in Fig. 7 are also listed in Table 2.

The slow phase reaction (absorbance increase part) in Fig. 5 stems most likely from the substitution of coordinated chloride in *cis*-$[Pt(NH_3)_2Cl_2]$ by excess thiosulfate, since thiosulfate is a good nucleophile. A plot of the observed rate constant k_s as a function of $[S_2O_3^{2-}]$ is illustrated in Fig. 8; within experimental error, the relation in Fig. 8 can be expressed by Eq. (7):

$$k_s = k_0 + k_1\left[S_2O_3^{2-}\right] \quad (7)$$

where $k_0 = -1.5 \pm 0.5\ s^{-1}$ and $k_1 = 0.76 \pm 0.06\ M^{-1}\ s^{-1}$ at 25.0 °C (pH 7.34 phosphate buffer and $\mu = 1.0$ M). The value of k_0 is not well determined due to the large error and thus is negligible. A mechanistic picture is outlined in Scheme 2 to account for the biphasic character observed for the reaction of *cis*-$[Pt(NH_3)_2Cl_2]$ with thiosulfate. Comparing reaction (4) with Scheme 2, we have **A** = *cis*-$[Pt(NH_3)_2Cl_4]$, **B** = *cis*-$[Pt(NH_3)_2Cl_2]$, and **C** = *cis*-$[Pt(NH_3)_2Cl(S_2O_3)]^-$.

Interaction of $[Pt(dach)Cl_4]$ with thiosulfate

The reaction of $[Pt(dach)Cl_4]$ with thiosulfate was monitored at 285 nm, and the kinetic traces also showed a biphasic character, namely a fast reaction followed by a slow reaction. The fast reaction was analogously assigned to the reduction of $[Pt(dach)Cl_4]$ to $[Pt(dach)Cl_2]$, while the slow reaction was ascribed to the substitution of chloride in $[Pt(dach)Cl_2]$ by excess thiosulfate. In this case, only the reduction was measured and demonstrated to follow second-order kinetics (Fig. 6); rate constants and activation parameters were evaluated (Fig. 7; Table 2). Scheme 2 can also be used to interpret the biphasic reaction character of $[Pt(dach)Cl_4]$.

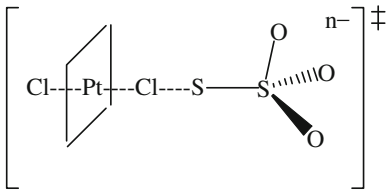

Scheme 3 *trans*-$[PtCl_2(CN)_4]^{2-}$, $n = 4$; *cis*-$[pt(NH_3)_2Cl_4]$ and $[Pt(dach)Cl_4]$, $n = 2$

Electron transfer process

The reductions of anticancer prodrugs *cis*-$[Pt(NH_3)_2Cl_2]$ and $[Pt(dach)Cl_4]$ and of the model compound *trans*-$[PtCl_2(CN)_4]^{2-}$ by thiosulfate all follow an essentially identical rate law. Hence, the reductions are anticipated to proceed via a common mechanism. The rate-determining step can be regarded as a Cl^+ transfer from the Pt(IV) center to the attacking thiosulfate with a conceivable transition state as shown in Scheme 3.

In the transition state, the attack of thiosulfate on one of the axial chloride ligands will result in concurrent partial Cl–S bond formation and Cl–Pt–Cl bond cleavage. The partial Cl–S bond formation will make the activation entropies negative, whereas Cl–Pt–Cl bond breaking will give a positive contribution to the activation entropies. As a consequence, the small negative values of the activation entropies for all the three Pt(IV) complexes (Table 2) are consistent with the transition state delineated above. Previously, the rate-determining steps for the reductions of *trans*-dichloro-platinum(IV) anticancer prodrugs and model compounds by sulfur-containing molecules were also explained in terms of a Cl^+ transfer process [24–28].

Conclusions

The reduction of *trans*-$[PtCl_2(CN)_4]^{2-}$ by thiosulfate obeys an overall second-order rate law while the pH essentially has no influence on the reaction rate. In the reactions of *cis*-$[Pt(NH_3)_2Cl_4]$ and $[Pt(dach)Cl_4]$ with thiosulfate, a fast reduction is followed by a slow substitution on the intermediate Pt(II) complexes; the reduction rates of these processes can be measured separately. Thus, the second-order rate constants for the reduction of all the three Pt(IV) complexes were determined at pH 7.34 and several temperatures. The reduction of *cis*-$[Pt(NH_3)_2Cl_4]$ and $[Pt(dach)Cl_4]$ by thiosulfate proceed with similar rates, probably due to their similar configurations, whereas the reduction of *trans*-$[PtCl_2(CN)_4]^{2-}$ is about 1,000 times faster. The activation parameters for all the three complexes support a Cl^+ transfer from the platinum(IV) center to the attacking thiosulfate in the rate-determining step. Scheme 2 provides a detailed mechanism for the overall interactions of the prodrugs *cis*-$[Pt(NH_3)_2Cl_4]$ and $[Pt(dach)Cl_4]$ with thiosulfate. This information, together with the rate constants derived, should prove useful if sodium thiosulfate is considered to be a rescuing agent for Pt(IV) anticancer drugs.

Acknowledgments Financial support to this work by grants from the Natural Science Foundation of Hebei University (2012ZD01) and from the Youth Foundation of Hebei Educational Committee (Q2012058 and Z2012041) is acknowledged.

References

1. Wheate NJ, Walker S, Craig GE, Oun R (2010) Dalton Trans 39:8113–8127
2. Wexselblatt Z, Gibson D (2012) J Inorg Biochem 117:220–229
3. Casini A, Reedijk J (2012) Chem Sci 3:3135–3144
4. Brock PR, Knight KR, Freyer DR, Campbell KCM, Steyger PS, Blakley BW, Rassekh SR, Chang KW, Fligor BJ, Reajput K, Sullivan M, Neuwelt EA (2012) J Clin Oncol 30:2408–2417
5. Sooriyaarachchi M, Narendran A, Gailer J (2012) Metallomics 4:960–967
6. Doolittle ND, Muldoon LL, Brummett RE, Tyson RM, Lacy C, Bubalo JS, Fraemer DF, Heimrich MC, Henry JA, Neuwelt EA (2001) Clin Cancer Res 7:493–500
7. Muldoon LL, Pagel MA, Kroll RA, Brummett RE, Doolittle ND, Zuhowski EG, Egorin MJ, Neuwelt EA (2000) Clin Cancer Res 6:309–315
8. Elferink F, van der Vijgh WJF, Klein VI, Pinedo HM (1986) Clin Chem 32:641–645
9. Leeuwenkamp OR, van der Vijgh WJF, Neijt J, Pinedo HM (1990) Cancer Chemother Pharmacol 27:111–114
10. Videhult P, Laurell G, Wallin I, Ehrsson H (2006) Exp Biol Med 231:1638–1645
11. Shi T, Rabenstein DL (1999) J Org Chem 64:4590–4595
12. Shi T, Rabenstein DL (2000) J Am Chem Soc 122:6809–6815
13. Shi T, Rabenstein DL (2001) Tetrahedron Lett 42:7203–7206
14. Shi T, Rabesntein DL (2002) Bioorg Med Chem Lett 12: 2237–2240
15. Shi T, Spain SM, Rabenstein DL (2006) Angew Chem Int Ed 45:1780–1783
16. Narayan M, Welker E, Wanjalla C, Xu C, Scheraga HA (2003) Biochemistry 42:10783–10789
17. Shi T, Elding LI (1998) Inorg Chim Acta 282:55–60
18. Drougge L, Elding LI (1986) Inorg Chim Acta 121:175–183
19. Anderson WK, Quagllato DA, Haugwitz RD, Narayanan VL, Wolpert-DeFilippes MK (1986) Cancer Treat Rep 70:997–1002
20. Lamprecht GJ, Leipoldt JG, Dennis CR, Basson SS (1980) React Kinet Catal Lett 13:269–275
21. Bhattacherya S, Ali M, Gangopadhyay S, Banerjee P (1996) J Chem Soc Dalton Trans 2645–2651
22. Chandayot P, Fanchiang YT (1985) Inorg Chem 24:3532–3534
23. Espenson JH (1995) Chemical kinetics and reaction mechanisms, 2nd edn, Chapter 4. McGraw-Hill, New York
24. Shi T, Berglund J, Elding LI (1996) Inorg Chem 35:3498–3503
25. Shi T, Berglund J, Elding LI (1997) J Chem Soc Dalton Trans 2073–2077
26. Lemma K, Shi T, Elding LI (2000) Inorg Chem 39:1728–1734
27. Huo S, Shen S, Liu D, Shi T (2012) J Phys Chem B 116: 6522–6528
28. Huo S, Shi H, Liu D, Shen S, Zhang J, Song C, Shi T (2013) J Inorg Biochem 125:9–15